

Single and double electron capture from He by Ar¹⁶⁺ studied using cold-target recoil-ion momentum spectroscopy

M. A. Abdallah, W. Wolff,* H. E. Wolf,* E. Y. Kamber,† M. Stöckli, and C. L. Cocke
J.R. Macdonald Laboratory, Physics Department, Kansas State University, Manhattan, Kansas 66506

(Received 24 April 1998)

Single and double electron capture from He targets by Ar¹⁶⁺ ions have been studied at projectile velocities from 0.3 to 1.5 a.u. Cold-target recoil-ion momentum spectroscopy was used to record the energy gain and scattering angle simultaneously. For single capture, the reaction window is found to spread in width approximately as the square root of the projectile velocity and to shift slightly toward smaller energy-gain values as the velocity increases. The angular distributions center at the half Coulomb angle over most of the velocity range covered, but differ in shape from multichannel Landau-Zener model results. For double capture, transfer ionization dominates and feeds primarily n -symmetric states, where n is the principal quantum number. True double capture feeds mainly n -asymmetric states. The angular distributions for double capture lie outside the half Coulomb angle, indicating the importance of two-step processes in populating doubly excited states. [S1050-2947(98)05610-8]

PACS number(s): 34.70.+e, 34.50.Fa

I. INTRODUCTION

Electron capture by multiply charged ions from the two-electron target He has been heavily studied over more than a decade. At low velocities, it is well established that single capture takes place at large internuclear distances, between 6 and 10 a.u. typically, leading to very selective final-state population of only one or two n values [1–4]. Rather successful modeling of the process has been formulated in terms of classical barrier [5,6], multichannel Landau-Zener (MCLZ) [2,7] and classical trajectory Monte Carlo (CTMC) [8,9] languages. For low-charged projectiles, very good descriptions of such collisions through coupled-channel calculations, even including the differential cross sections, are available [10,11]. For highly charged projectiles, however, such accurate descriptions cease to be feasible because of the very large number of final channels that must be considered and simple models remain useful.

Double capture usually populates doubly excited states on the projectile at internuclear distances similar to, or slightly inside, the single-capture radii, with n values near or slightly below those populated in single capture. A great deal of discussion has focused on the role of “correlated” capture, involving two-electron matrix elements, which can populate doubly excited states with quite different n values [1,4,12–14]. While doubly excited states characterized by electrons in similar n values tend to decay rapidly through autoionization, leaving a doubly charged target but a projectile retaining only one captured electron [transfer ionization (TI), also known as autoionizing double capture], states with very different n have a much better chance to radiatively stabilize, leading to true double capture (TDC).

In this paper we use cold-target recoil-ion-momentum

spectroscopy (COLTRIMS) [15–17] to study low-energy capture by highly charged ions from He. This technique allows the simultaneous investigation of the final-state distributions, giving information on the behavior of the reaction window, and angular distributions for each final state, giving information on the capture mechanisms. In the low-velocity region, this technique has been used previously by two other groups [18–21] and by us [22] to study capture from He by high- Z projectiles. A particularly important aspect of this approach is that it allows high-resolution studies, with good statistics, to be carried out over a wide range of projectile velocities. In the present case, we go from 0.3 a.u., clearly in the classical-barrier “slow” region, to 1.5 a.u., which is definitely entering the transition region where neither energy- nor momentum-matching criteria are adequate alone to describe the main characteristics of the capture. The projectile used here is Ar¹⁶⁺, which appears to the He to be a scantily clad nucleus, nearly a point charge. In contrast to lower charged projectiles such as Ar⁸⁺, whose COLTRIMS study we recently reported [22], the final states populated on the Ar¹⁶⁺ core are nearly hydrogenic and the subshell splitting is unresolvable, being typically of the order of tens of meV. Complete coupled-channel calculations are presently impossible for such a system due to the large number of open channels.

Several previous studies of Ar ^{q +} on He for q near 16 have been reported in the low-velocity region. Total cross sections and energy gain measurements for highly charged projectiles, including Ar¹⁶⁺, on He were measured by Iwai *et al.* [23] and Tawara *et al.* [24], who concluded that the correlation between the cross section and energy gain was approximately that to be expected from Coulomb potential curves for high q . Vancura *et al.* [25] measured absolute cross sections for capture from He by $8 < q < 16$, to which subsequent partial cross-section measurements have been normalized. Wu *et al.* [26,27] used a low-resolution form of recoil momentum spectroscopy to measure cross sections, average Q values (where Q is the electronic energy release),

*Present address: Instituto de Fisica, Universidade Federal do Rio de Janeiro, Caixa Postal 68.528, 21945-970 Rio de Janeiro, Brazil.

†Present address: Physics Department, Western Michigan University, Kalamazoo, MI 49008.

and angular distributions for capture by Ar^{16+} from He for $0.19 < v < 1.55$ a.u. They found that the average Q value actually decreased with increasing v , a counterintuitive effect that we are able to illuminate further in this paper. The most complete previous experiment on the system studied here was carried out by Cederquist *et al.* [28], who measured translational energy gain spectra for $3.35q$ -keV Ar^{15-18+} on He and deduced final-state populations for single- and double-capture channels. High-resolution COLTRIMS spectra for Ar^{18+} on He were reported by Cassimi *et al.* at 6.75 keV/nucleon [20] and information on final-state distributions and angular distributions was deduced for single capture.

II. EXPERIMENT

The Ar^{16+} ions were produced by the Kansas State University electron beam ion source and accelerated to voltages between 10 and 150 kV. The COLTRIMS apparatus is described in some detail in Ref. [22], to which the reader is referred for more detail. Briefly, the beam crossed a supersonically cooled He jet with an internal temperature below 1 K. The recoil He ions produced by capture were impelled onto the face of a two-dimensional (2D) position-sensitive channel-plate detector (PSD) by a slightly focusing transverse electric field, while the charge-state-analyzed projectiles were detected in coincidence with the recoils by a second 2D PSD. Single capture was identified as a coincidence between He^+ and Ar^{15+} ions. Transfer ionization and true double capture were identified as coincidences between He^{2+} recoils and Ar^{15+} and Ar^{14+} projectiles, respectively. The overall recoil momentum resolution was between 0.2 and 0.4 a.u., depending on the specific run and settings of the extraction field. Count rates were such that most spectra shown in the paper took typically less than 1 h to accumulate.

III. RESULTS

A. Single capture

1. Q -value spectra

Figure 1 shows density plots of longitudinal versus transverse recoil momenta for single capture at the lowest and highest projectile velocities used. The longitudinal momentum p_z has been converted into a Q value using

$$Q = -vp_z - n_t v^2/2, \quad (1)$$

where v is the projectile velocity and n_t the number of electrons transferred [29]. All quantities in this equation are expressed in a.u. The qualitative behavior is as expected, with capture to successively more tightly bound final states (higher energy release) requiring more transverse momentum transfer. In Fig. 2 we show Q -value spectra for all measured velocities, obtained by projecting spectra such as shown in Fig. 1 onto the longitudinal momentum-transfer axis. At the lowest v , the overwhelmingly dominant population of $n=7$ is observed. This result is in agreement with the expectations of either a classical barrier model [6] (which gives $n=7.3$) or a MCLZ model [30,2]. It is also in good agreement with the observations of Cederquist *et al.*, but in disagreement with

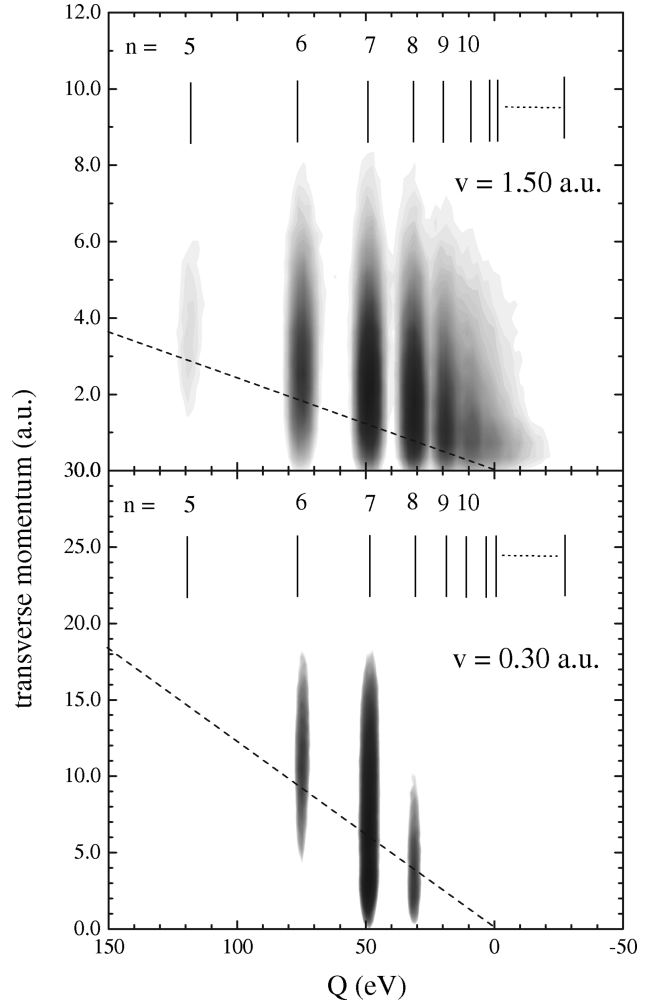


FIG. 1. Density plot showing the transverse momentum transfer to the recoil versus the Q value for two values of the projectile velocity v , for the single-capture channel. The Q value was deduced from the longitudinal momentum transfer. The dashed line shows the location of the half Coulomb angle θ_c (see the text).

the average Q -value measurements of Wu *et al.* [26]. The present resolution is much better than that of Wu *et al.* and allows unambiguous resolution of the final principal n , so there can be little question that the present results are correct. As the projectile velocity increases, the reaction window is seen to spread, with a particularly strong increase in the population of higher n states. On the basis of a Landau-Zener argument, one might expect that lower n states would gain importance as v increases, as distant crossings become increasingly diabatic and inner ones less adiabatic. In Fig. 3 we compare our experimental population distributions with MCLZ predictions and find that this model accounts for some aspects of the data, especially in predicting the decrease of the relative population of $n=7$ as v increases. However, the model completely fails to predict the increasing importance of high n populations. The most important effect of raising v is to spread, rather than shift, the reaction window. Since the density of states at higher n is much larger than that for low n , the result is to shift the centroid of the reaction window to lower, not higher, Q , as can be seen in Fig. 4, where we plot the average Q value for

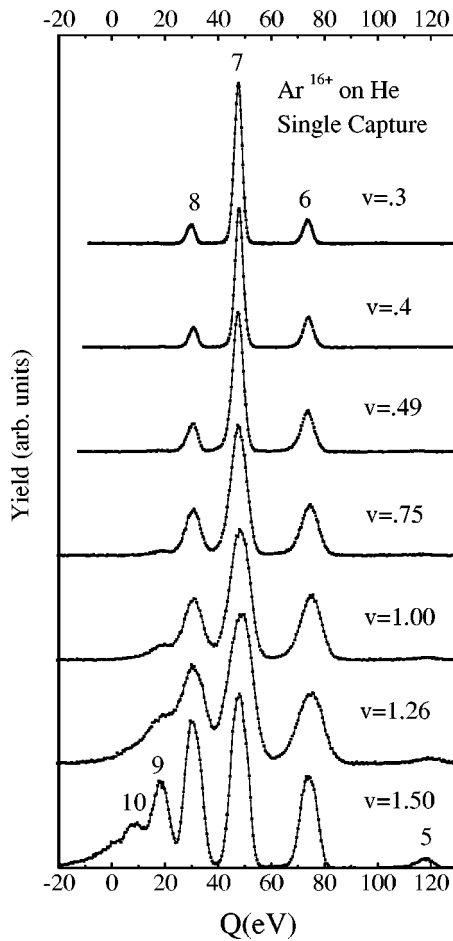


FIG. 2. Q -value plots for single capture for various values of the projectile velocity v (in a.u.).

single capture versus v . A similar effect was seen by Wu *et al.* [26,27]. Although the resolution in that experiment did not allow a clear illumination of how this occurred, it was speculated that the increasing population of higher n was due in part to the increasing angular momentum transferred in the collision as v is increased, enabling the population of high n and l , which have high statistical weight. A similar effect was seen by Abdallah *et al.* [22] for Ar^{8+} on He and it is now clear that this trend is probably quite general as the projectile velocity goes from the capture-dominated into the ionization-dominated velocity regime. It is known, and was confirmed experimentally by Wu *et al.* [27] as well as by CTMC calculations presented in that work, that eventually low n states will again dominate, but this does not happen until v/q becomes the order of unity (where v is expressed in a.u. and q is the projectile charge state). For the present system, this requires v of the order of 16 a.u. or a beam energy of more than 200 MeV.

Figure 4 also shows explicitly that the width of the reaction window depends much more strongly on v than does the average Q value. While many capture studies over the past two decades have shown v -dependent population distributions, few experiments have been reported with sufficiently high q to avoid complications due to nonsmooth final-state distributions or with a sufficiently large range of v to allow quantitative investigation of this point. One would expect, on simple uncertainty-principle grounds, that the reaction win-

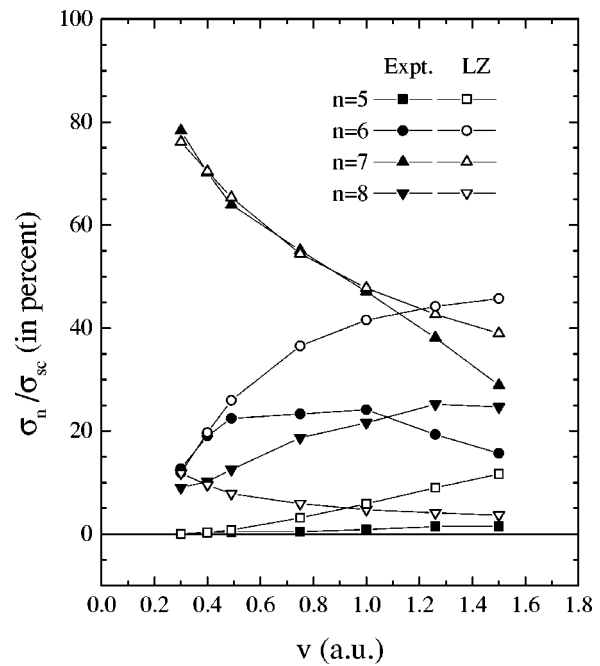


FIG. 3. Experimental populations distributions versus the projectile velocity v (closed symbols), compared with population distributions predicted from the Landau-Zener model (open symbols).

dow might spread roughly according to $\Delta E \Delta t = \hbar$. Niehaus [6] used such an argument to deduce an explicit expression for the width of the reaction window as a function of projectile velocity. His approach is reminiscent of the use of the uncertainty principle by Bohr and Lindhard [31] for the determination of the criterion for the use of classical trajectories in atomic collisions, except that uncertainty principle is used in its energy-time form. Briefly, one can define a classical energy width

$$\Delta E_c = (dV/dR)\Delta R, \tag{2}$$

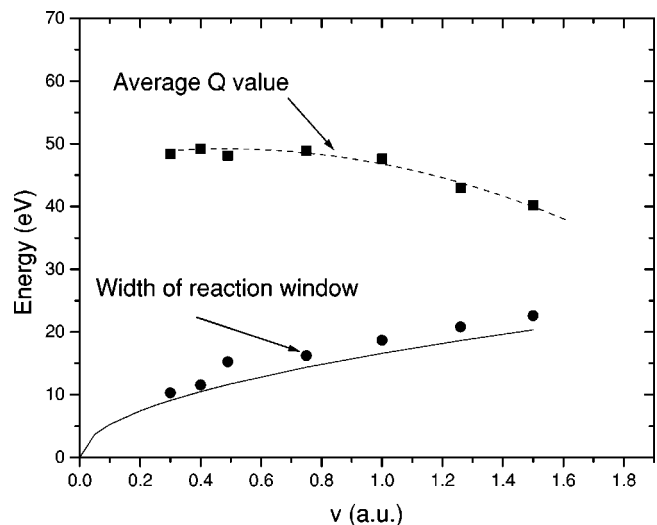


FIG. 4. Average Q value (closed squares) and width of the Q window (closed circles) plotted vs the projectile velocity v . The dashed line is to guide the eye, while the solid line is from Eq. (5) (see the text).

where V is the energy separation of the crossing curves and ΔR is some characteristic distance over which the transition is assumed to occur. A quantum mechanical energy width can be defined by

$$\Delta E_Q = \hbar v / \Delta R. \quad (3)$$

If one now defines the total energy width to be the quadratic combination of these two and chooses the value of ΔR that minimizes this width, one obtains

$$\Delta E = \sqrt{2v dV/dR}. \quad (4)$$

This result differs from that of Niehaus by $\sqrt{2}$. If we apply this to the present case, evaluating dV/dR from a Coulomb potential curve for Ar^{15+} receding from He^+ at the crossing radius of 9 a.u., we obtain

$$\Delta E \text{ (eV)} = 16.6\sqrt{v \text{ (a.u.)}}. \quad (5)$$

This result is shown as a solid curve in Fig. 4 and is in remarkable agreement with the measured reaction window width. This agreement must be considered to be somewhat fortuitous, in view of the roughness of the estimate, but the dependence on \sqrt{v} seems to be confirmed. Fisher *et al.* [32] have recently observed a similar spreading of the reaction window with increasing v for capture from Rydberg states by multiply charged ions. They find that CTMC calculations predict nearly exactly the trend that they observe, which raises the interesting question as to how CTMC calculations provide information about \hbar [33].

2. Angular distributions

The transverse momenta spectra for single capture are shown in the density plots of Fig. 1 and as separate angular distributions in Fig. 5. In the localized curve-crossing picture for capture, the angular deflection in the laboratory system of a projectile undergoing capture at an impact parameter equal to the crossing radius is given by the half Coulomb angle $\theta_C = Q/2E$, where E is the projectile laboratory energy. The transverse momentum transfer (p_t) is related to the scattering angle by

$$p_t = p_0 \theta, \quad (6)$$

where p_0 is the momentum of the incident projectile. Therefore a plot of p_t versus Q is a straight line, which is shown as a dashed line in Fig. 1. In Fig. 5 this θ_C will occur at an $E\theta$ value of $Q/2$ and this is shown as a thin vertical line for each final n . As discussed by several authors [30,34–37], capture along semiclassical trajectories in curve-crossing space will produce deflection angles greater than (less than) θ_C for capture on the way in (out), respectively. Since for optimum adiabaticity, which roughly holds for the strongest final channel, the transfer probability is nearly one-half, this leads to angular distributions characterized by roughly equal cross sections lying inside and outside θ_C . This expected trend is seen to be rather well borne out for low velocities in Figs. 1 and 5, but the data begin to depart rather firmly to larger scattering angles by the time $v = 1.5$ is reached. This peaking of the distributions near θ_C was also observed by Cassimi *et al.* [20] for Ar^{18+} at low velocities. For lower q , coupled-

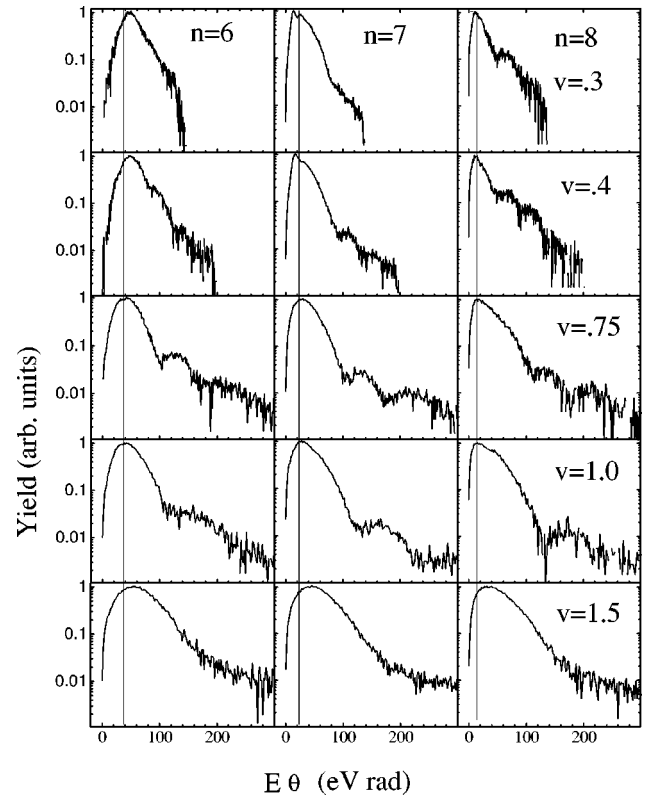


FIG. 5. Angular distributions for single capture for various final n values and projectile velocities v . The vertical solid lines denote the locations of the half Coulomb angles θ_C .

channel calculations have been found to give an excellent description of single capture [11,22], but such calculations are not feasible for this case and we retreat to model analyses. A comparison of the data with the MCLZ calculation of Andersson *et al.* [30] is shown in Fig. 6. In this case the calculation is carried out using the coupling matrix elements of Olson and Salop [38] with no modification for subshell splitting. As discussed for other cases, this model gives deflection angles of the correct general magnitude, but fails to reproduce the shape of the observed spectra. A similar result was found in Refs. [22] and [39]. Although we have not made such a comparison here, Duponchel [39] found that CTMC calculations were able to give a reasonable description of the angular distributions for similar systems.

The small statistical error bars on the angular distributions allow us to observe a feature previously unnoticed in such collisions, namely, an insistent and regular large-angle oscillation suggestive of simple diffraction. The effect appears in many of the spectra of Fig. 5, particularly strongly, for example, for $v = 0.75$ a.u., and is remarkably stable in oscillation frequency even for different final n values. We have no definite interpretation of this phenomenon, but speculate that it could be due to interference between trajectories in curve-crossing space associated with potential curves for different n values. In the following we argue that one might expect that the angular oscillation frequency would be independent of v if plotted versus transverse momentum transfer. For this reason, we replot in Fig. 7 selected angular distributions in this form. As discussed by many authors [40–43], an oscillation in transverse momentum transfer with period Δp_t can

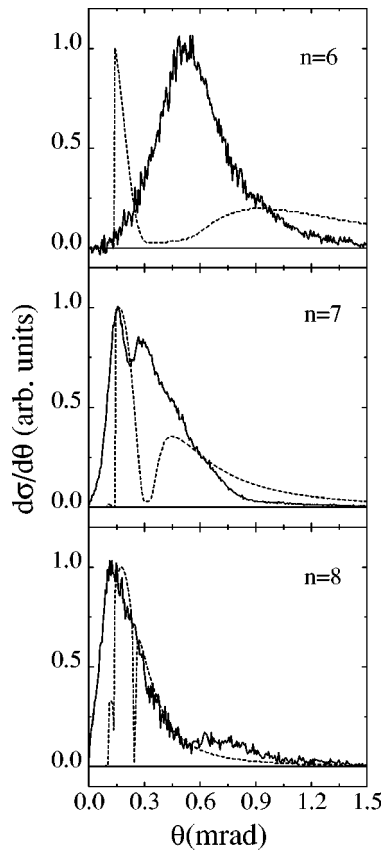


FIG. 6. Comparison of experimental angular distributions for a projectile velocity $v=0.3$ a.u. (continuous curves) with multichannel Landau-Zener model predictions (dashed curves) for the three major n values. Both experimental and model curves have been normalized to a peak value of unity.

be caused by a multibranch semiclassical deflection function if the branches are nearly parallel but shifted in impact parameter relative to each other by Δb , where Δb and Δp_t are related by

$$\Delta b \Delta p_t = h. \quad (7)$$

Estimating Δp_t from Fig. 7 as 7 a.u. leads to a Δb of 0.9 a.u. If one uses Coulomb potential curves, the resulting deflection functions for states of different n , for the case where n is large so that several different n values lie within the reaction window, will be very similar in shape and shifted with respect to each other in impact parameter by the separation between their crossing radii. For example, for the present case, Δb would be 2.1 and 2.3 a.u. for interference between trajectories involving adjacent deflection functions for n and n' of 5,6 and 6,7, respectively. These values of Δb are somewhat, but not an order of magnitude, larger than the value of 0.9 a.u. We thus suspect that this kind of interference may lie behind the oscillations we observe. When many possible routes in curve-crossing space are possible, one usually expects that the various frequencies involved will wash out. It may be that this mechanism works only when such highly charged projectiles are used that the deflection functions for adjacent n are shifted relative to each other by a rather constant amount for all important n . That the oscillations are visible only at larger angles suggests that they

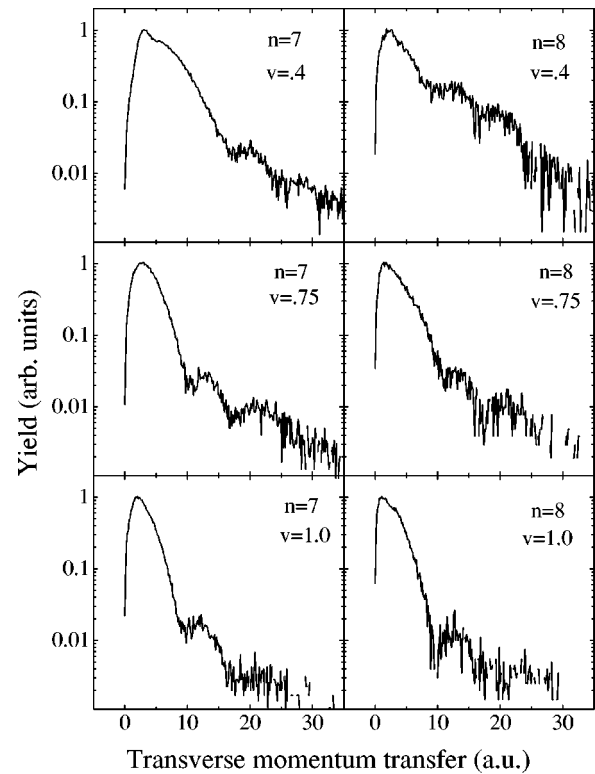


FIG. 7. Selected angular distributions for several values of the final n and projectile velocity v , plotted vs the transverse momentum transfer, showing a regular diffractionlike structure at large angles.

might be associated with crossings at small b , which might not be the determining ones for the total cross section and for which Δb is smaller. The angular region in which the oscillations occur makes a negligible contribution to the total cross section. This is all rather speculative and would have to be confirmed by, for example, a coupled-channel calculation in order to be elevated to the status of a convincing explanation.

B. Double capture

It is well established that capture of two electrons by slow, highly charged projectiles nearly always leads to the population of doubly excited states, which very often decay through autoionization processes leading to a doubly charged recoil ion accompanied by a projectile that has retained only one electron (TI). If the doubly excited state radiatively stabilizes, the projectile retains both electrons, resulting in TDC. The radiative stabilization tends to be more probable when the doubly excited state is characterized by electrons with very different principal quantum numbers (asymmetric states). While symmetric states are often easy to populate through two sequential crossings with single capture channels, the asymmetric states are not, and the mechanisms for their population have been the center of considerable discussion in the literature for several years (see, e.g., Refs. [1,4,12,13] and references cited therein). These mechanisms include direct both dielectronic two-electron transitions driven by the electron-electron interaction [13,44,45] and autotransfer to Rydbergs (ATR) [46] whereby long-range cou-

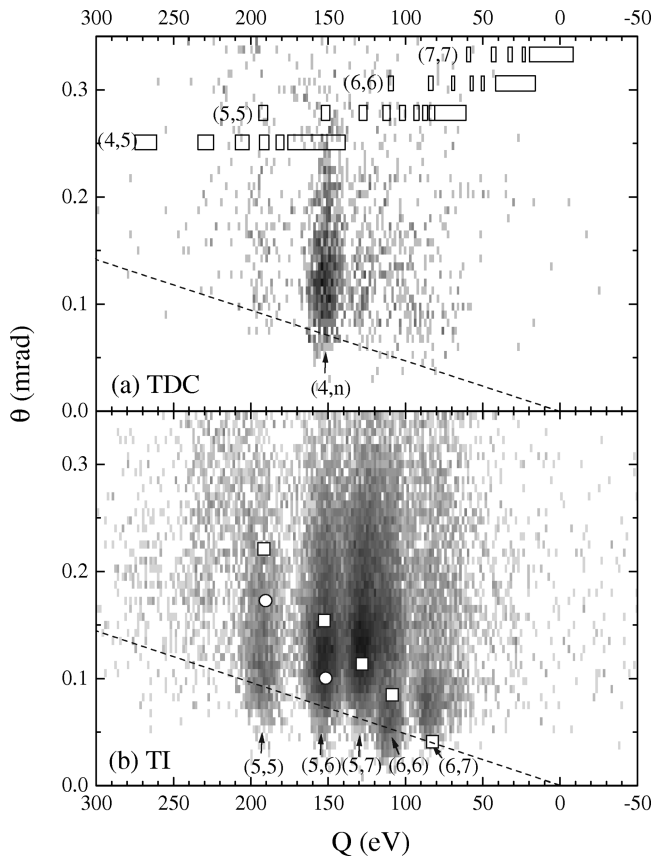


FIG. 8. Density plot showing the effective scattering angle of the projectile vs the Q value for a projectile velocity $v=1$ a.u. The Q value was deduced from the longitudinal momentum transfer and the scattering angle from the transverse momentum transfer. (a) and (b) show the true-double-capture (TDC) and transfer ionization (TI) channels, respectively. The dashed lines show the locations of the half Coulomb angle θ_C . The energies expected [28] for capture to a final configuration (n,n') are shown above (a) and identifications of the observed lines are denoted in the bottom of each figure by (n,n') . The small open circles and squares indicate the calculated deflection angles for two-step transitions, with $n=7$ and $n=6$, respectively, as the enabling first-step single-capture transition (see the text).

plings can transfer population from symmetric configurations into asymmetric ones that are nearly degenerate on the way out of the collision.

1. Q -value spectra

In Fig. 8 we show density plots similar to those of Fig. 1, but for the TI and TDC channels, for $v=1$ a.u. Expected energies for doubly excited series, taken from [28], are shown above the TDC figure. These spectra are projected onto the Q -value axis and shown for several projectile velocities in Fig. 9. The density of doubly excited states is high, but general identifications of the populations are nevertheless possible. The TI, which carries more than 70% of the double-capture strength for all v , populates most strongly the $(n,n')=(6,7)$, $(6,6)$, $(5,7)$, $(5,6)$, and $(5,5)$ channels. These states cross the incident channel only slightly inside the active range for single capture and would be expected to be strongly populated. A multichannel classical barrier calculation [6] predicts the population of $(6,7)$, in fair agree-

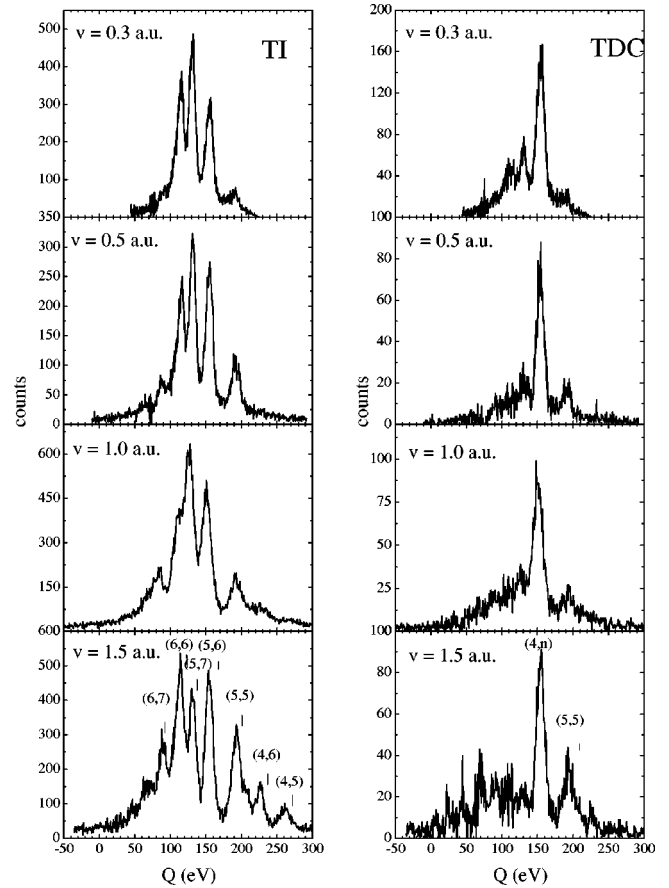


FIG. 9. Q -value plots for transfer ionization (left-hand column) and true double capture (right-hand column) for various values of the projectile velocity v .

ment with this result. The average Q value for TI lies near 130 eV, about 40 eV lower than that found by Wu *et al.*, but in agreement with the results of Cederquist *et al.* [28]. Since the individual states are resolved and identified here, there can be little argument that the present values are to be preferred over those of Wu *et al.* A similar Q scale shift for single capture was noted earlier. In the absence of resolvable lines, as was the case in the work of Wu *et al.*, it is very difficult to establish the absolute zero in the longitudinal momentum transfer and we believe that this error caused an error in absolute Q value in that work. The trend of Q with v established in that work remains valid however.

The TDC, which carries typically only about 20% of the capture strength, is seen to populate mainly a group near $(n,n')=(5,6)$ or $(4,n')$ where n' is very large. We believe that the major population is of the asymmetric series $(4,n')$, which would be expected to have a large radiative stabilization probability. As the projectile velocity is raised, the major effect is to broaden the reaction window, as for single capture, strengthening the population of other configurations, especially those with lower n and more inner crossings.

2. Angular distributions and population mechanisms

In Fig. 8 we show the expected location of values of θ_C for double capture as solid lines. In contrast to the situation for single capture, it is seen that nearly all double capture

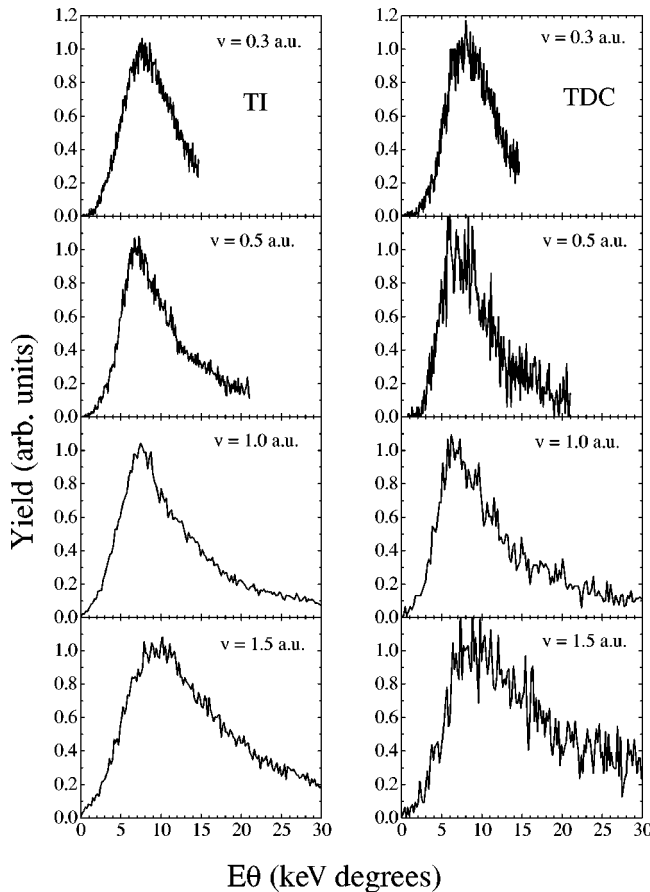


FIG. 10. Summed angular distributions for TI and TDC for various values of the projectile velocity v .

results in deflection angles larger than the θ_C . A similar result was seen by Flechard *et al.* for Ne^{10+} on He [21]. Such an effect is expected since double capture does not dominantly occur in a single transition in the crossing of the incident channel with the outgoing channel, but more commonly occurs through couplings with single-capture channels that require at least one capture on the way in. We note that this generalization even applies to the population of the $(4, n')$ series in TDC, which is characterized by transverse momentum transfers very similar to those for the population of the nearly degenerate $(5, 6)$ and $(5, 7)$ configurations. Thus the data show no evidence for radically different trajectories in curve-crossing space for the population of symmetric and asymmetric configurations. This is also seen in Fig. 10, where we show total angular distributions, summed over all final channels, for TDC and TI. The observed behavior would be expected if the population of the $(4, n')$ series proceeded through any kind of mixing, including both ATR and transient configuration mixing during the collision. There is certainly no evidence in the angular distributions that the $(4, n')$ series is populated in a single direct correlated excitation-transfer process at a crossing with the incident channel.

We have used Coulomb potential curves, shown in Fig. 11, and classical trajectories to estimate the scattering angles at which the TI channels would be expected to maximize if the population of these configurations proceeded through a two-step process. Such curves are good approximations to

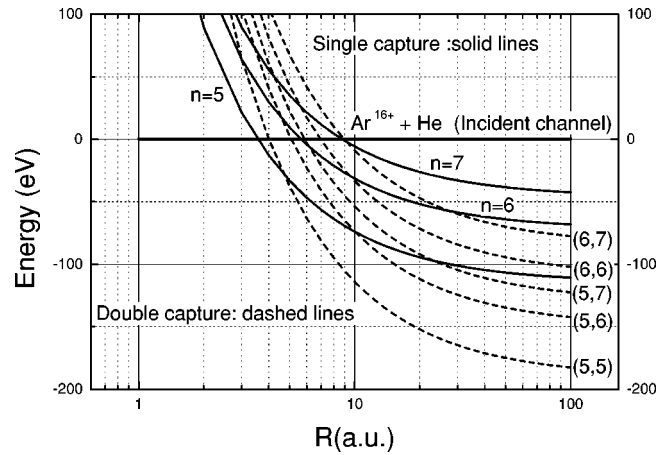


FIG. 11. Coulomb potential curves for single and double capture. For simplicity, the polarization energy in the incident channel is not included.

the diabatic potential curves for this system. For simplicity, we choose not to include the polarization interaction between the projectile and the He in the incoming channel; inclusion of this potential would shift all crossing radii to slightly smaller values. Our approach is similar to that of Flechard *et al.* [21]. The path in curve-crossing space on the way in was assumed to follow the $n=7$ single-capture curve from the first crossing with the incident channel to the crossing with the final double-capture curve. We take $n=7$ as the promoter potential curve for all final channels, even those that do not populate configurations in which $n=7$ appears, because the behavior of the system at this curve crossing is likely to be rather adiabatic (this is the strongest single-capture channel). The path on the way out is taken to be on the appropriate double-capture curve. The two-step deflection angles were calculated as the sum of the deflections accumulated over these potential curves for an impact parameter equal to the radius at which the $n=7$ curve crosses the double-capture curve. The results from this prescription are shown in Fig. 8 as squares for the population of the $(n, n') = (6, 7)$, $(6, 6)$, $(5, 7)$, $(5, 6)$, and $(5, 5)$ final configurations. For the last two of these, population along the $n=6$ single-capture path would also have been possible: The corresponding deflection angles are shown as open circles in Fig. 8 and there is evidence that this path is important for these cases. These deflection angles are in rather good agreement with the observed angular maxima. If instead of allowing $n=7$ to be a universal promoter we had insisted on strict conservation of n in two-step processes, we would have obtained much smaller scattering angles. For example, the configuration $(6, 6)$ could be populated through a crossing with $n=6$ in the way in and the $(6, 6)$ on the way out. However, the scattering angle calculated for such a process is only 0.4 mrad, much too small to be consistent with the data. In general, if there is not promotion on a single-capture curve on the way in, the calculated deflection angle will be too small. We thus believe that a correct picture of the collision is that the population follows the $n=7$ and to a lesser extent the $n=6$ curve on the way in and that these channels then couple to the various doubly excited states in the inner region without strict conservation of principal quantum number.

IV. SUMMARY AND CONCLUSIONS

We have used COLTRIMS to measure high-resolution two-dimensional momentum spectra in which the Q value (longitudinal momentum transfer) and scattering angle (transverse momentum transfer) are resolved simultaneously for single and double capture from He by Ar^{16+} projectiles. We have done this over a range of impact velocities extending from the slow, classical-barrier region into the region where appreciable reaction window spreading is seen. For single capture, a good understanding of the Q -value distributions at low v is established. The spread of the reaction window with v is remarkably well described by a simple model based on the energy-time uncertainty principle, perhaps fortuitously so. The angular distributions are also observed to spread outside the slow-collision values as v is raised and no model explanation for this is at hand. An insistent diffraction structure is seen in the angular distributions at large scattering angles and only a speculative explanation is suggested. For double capture, the population of

symmetric (n, n') is observed to lead to transfer ionization, whereas the population of asymmetric ($4, n'$) states leads to radiative stabilization. The angular distributions suggest that two-step processes dominate the double capture. There is no essential difference in the angular distributions for the population of symmetric and asymmetric states. In contrast to lower charged projectiles for which coupled-channel calculations are feasible, model explanations seem still to be required for such highly charged systems. Such a model approach is particularly inadequate in dealing with the velocity dependence of characteristics of the reaction.

ACKNOWLEDGMENTS

This work was supported by the Division of Chemical Sciences, Basic Energy Sciences, Office of Energy Research, U.S. Department of Energy. We thank E. Sidky and C. D. Lin for helpful discussions. We thank A. Bárány for sending us the program of L. Andersson with which the Landau-Zener calculations were performed.

-
- [1] M. Barat and P. Roncin, *J. Phys. B* **25**, 2205 (1992).
 [2] E. K. Janev and H. Winter, *Phys. Rep.* **117**, 265 (1985).
 [3] E. K. Janev and L. P. Presnyakov, *Phys. Rep.* **70**, 1 (1981).
 [4] C. L. Cocke, in *Review of Fundamental Processes and Applications of Atoms and Ions*, edited by C. D. Lin (World Scientific, Singapore, 1993), p. 111.
 [5] H. Ryufuku, K. Sasaki, and T. Watanabe, *Phys. Rev. A* **21**, 745 (1980).
 [6] A. Niehaus, *J. Phys. B* **19**, 2925 (1986).
 [7] C. Zener, *Proc. R. Soc. London, Ser. A* **137**, 696 (1932); L. D. Landau, *Phys. Sovietum* **2**, 46 (1932).
 [8] R. E. Olson, *Phys. Rev. A* **24**, 1726 (1981).
 [9] B. H. Bransden and M. R. C. McDowell, *Charge Exchange and the Theory of Ion-Atom Collisions* (Clarendon, Oxford, in press).
 [10] W. Fritsch, in *Review of Fundamental Processes and Applications of Atoms and Ions* (Ref. [4]), p. 239.
 [11] W. Fritsch and C. D. Lin, *Phys. Rev. A* **54**, 4931 (1996).
 [12] N. Stolterfoht, C. C. Havener, R. A. Phaneuf, J. K. Swenson, S. M. Shafroth, and F. W. Meyer, *Phys. Rev. Lett.* **57**, 74 (1986).
 [13] N. Stolterfoht, C. C. Havener, R. A. Phaneuf, J. K. Swenson, S. M. Shafroth, and F. W. Meyer, *Nucl. Instrum. Methods Phys. Res. B* **27**, 584 (1987).
 [14] J.-Y. Chesnel, B. Sulik, H. Merabet, C. Bedouet, F. Fremont, X. Husson, M. Grether, A. Spieler, and N. Stolterfoht, *Phys. Rev. A* **57**, 3546 (1998).
 [15] J. Ullrich, R. Moshhammer, R. Dörner, O. Jagutzki, V. Mergel, H. Schmidt-Böcking, and L. Spielberger, *J. Phys. B* **30**, 2917 (1997).
 [16] J. Ullrich *et al.*, *Comments At. Mol. Phys.* **30**, 285 (1994).
 [17] R. Dörner (unpublished).
 [18] V. Mergel *et al.*, *Phys. Rev. Lett.* **79**, 387 (1997).
 [19] V. Mergel *et al.*, *Phys. Rev. Lett.* **74**, 2200 (1995).
 [20] A. Cassimi, S. Duponchel, X. Flechard, P. Jardin, P. Sortais, D. Hennecart, and R. E. Olson, *Phys. Rev. Lett.* **76**, 3679 (1996).
 [21] X. Flechard, S. Duponchel, L. Adoui, A. Cassimi, P. Roncin, and D. Hennecart, *J. Phys. B* **30**, 3697 (1997).
 [22] M. Abdallah, W. Wolff, H. E. Wolf, E. Sidky, E. Y. Kamber, M. Stöckli, C. D. Lin, and C. L. Cocke, *Phys. Rev. A* **57**, 4373 (1998).
 [23] T. Iwai, Y. Kaneko, M. Kimura, N. Kobayashi, A. Matsumoto, S. Ohtani, K. Okuno, S. Takagi, H. Tawara, and S. Tsurubuchi, *J. Phys. B* **17**, L95 (1985).
 [24] H. Tawara, T. Iwai, Y. Kaneko, M. Kimura, N. Kobayashi, A. Matsumoto, S. Ohtani, K. Okuno, S. Takagi, and S. Tsurubuchi, *J. Phys. B* **18**, 337 (1985).
 [25] J. Vancura, V. J. Marchetti, J. J. Perotti, and V. O. Kostroun, *Phys. Rev. A* **47**, 3758 (1993).
 [26] W. Wu, J. P. Giese, I. Ben-Itzhak, C. L. Cocke, P. Richard, M. Stöckli, R. Ali, H. Schöne, and R. E. Olson, *Phys. Rev. A* **48**, 3617 (1993).
 [27] W. Wu, Ph.D. dissertation, Kansas State University, 1994 (unpublished).
 [28] H. Cederquist, C. Biedermann, N. Selberg, and P. Hvelplund, *Phys. Rev. A* **51**, 2169 (1995).
 [29] M. R. C. McDowell and J. P. Coleman, *Introduction to the Theory of Atomic Collisions* (North-Holland, Amsterdam, 1970), p. 375.
 [30] L. Andersson, Research Institute of Physics, Stockholm, No. 86:2, 1986 (unpublished).
 [31] N. Bohr and J. Lindhard, *K. Dan. Vidensk. Selsk. Mat. Fys. Medd.* **28**, No. 7 (1954).
 [32] D. S. Fisher, C. W. Feherenbach, S. R. Lundeen, E. A. Hessels, and B. D. DePaola, *Phys. Rev. Lett.* **81**, 817 (1998).
 [33] S. Lundeen (private communication).
 [34] L. Andersson, H. Danared, and A. Bárány, *Nucl. Instrum. Methods Phys. Res. B* **23**, 54 (1987).
 [35] L. Tunnell, *et al.* *Phys. Rev. A* **35**, 3299 (1987).
 [36] L. Andersson *et al.*, *Phys. Rev. A* **43**, 4075 (1991).
 [37] C. Biedermann *et al.*, *Phys. Rev. A* **42**, 6905 (1990).
 [38] R. E. Olson and A. Salop, *Phys. Rev. A* **14**, 579 (1976).

- [39] S. Duponchel, Ph.D. thesis, University of Caen, 1997 (unpublished).
- [40] K. Ford and J. A. Wheeler, *Ann. Phys. (N.Y.)* **7**, 259 (1959).
- [41] F. T. Smith, *J. Chem. Phys.* **42**, 2419 (1965).
- [42] R. E. Olson and F. T. Smith, *Phys. Rev. A* **3**, 1607 (1971).
- [43] R. E. Olson and M. Kimura, *J. Phys. B* **15**, 4231 (1982).
- [44] N. Stolterfoht, *Phys. Scr.* **T46**, 22 (1993); **T51**, 39 (1994).
- [45] F. Fremont, H. Merabet, J.-Y. Chesnel, X. Husson, A. Lepoutre, D. Lecler, G. Rieger, and N. Stolterfoht, *Phys. Rev. A* **50**, 3117 (1994).
- [46] H. Bachau, P. Roncin, and C. Harel, *J. Phys. B* **25**, L109 (1992).